Natural convection enhancement in a porous cavity with Al_2O_3-Ethylene glycol/water nanofluids

A. Brusly Solomon, M. Sharifpur*, Tanja Ottermann, Carla Grobler, Michael Joubert and Josua P. Meyer

Department of Mechanical and Aeronautical Engineering, University of Pretoria, Pretoria 0002, South Africa

*Corresponding author

Dr. Mohsen Sharifpur,
Department of Mechanical and Aeronautical Engineering,
University of Pretoria,
Pretoria 0002,
South Africa.

Email: mohsen.sharifpur@up.ac.za
Telephone number: +27 12 420 2448 Fax number: +27 12 362 5124

Natural convection enhancement in a porous cavity with Al_2O_3-Ethylene glycol/water nanofluids

A. Brusly Solomon, M. Sharifpur*, Tanja Ottermann, Carla Grobler, Michael Joubert and Josua P. Meyer

Department of Mechanical and Aeronautical Engineering, University of Pretoria, Pretoria 0002, South Africa

Abstract

The natural convection heat transfer of a differentially heated cavity filled with porous material and saturated with nanofluid is studied. The nanofluid used in the present study contains 60% Ethylene glycol, 40% DI-water and 30 nm size Al_2O_3 nanoparticles. The volume concentration of nanofluid used is in the range of $0.05\% \leq \phi \leq 0.4\%$. The range of Rayleigh number in the present study is $1.2 \times 10^8 \leq Ra \leq 4 \times 10^8$ for clear cavity and $3 \times 10^3 \leq Ra \leq 1.3 \times 10^4$ for the porous cavity. Viscosity of the nanofluid is also measured at volume concentration of 0.05% and found one available model works for the calculations. In order to explain the heat transfer behaviour of the present system, heat transferred by both clear and porous cavity, heat transfer coefficients of both hot and cold wall, as well as Nusselt number variation with concentrations of nanofluids are presented. It is found that the performance of porous cavity filled with a nanofluid volume concentration of 0.05% is enhanced while the other concentrations of nanofluids deteriorate the performance. At a volume concentration of 0.05%, the heat transfer capability of porous cavity is enhanced to a maximum of 10% compared to the base fluids.

Keywords: Natural convection; porous cavity, nanofluids; Nusselt number; Al_2O_3, Ethylene glycol

1. Introduction

Natural convection heat transfer is one of the most fundamental heat transfer mechanism and it plays a major role in various industrial applications such as heat exchangers, energy storage, thermal management, solar collectors and food processing [1] etc. The natural convection process is driven by buoyancy forces that cause fluid motion. In general, thermo-physical properties of fluids play a major role in natural convection heat transfer as they influence the fluid motion through buoyancy forces. As the conventional heat transfer fluids have limitations in the heat transfer process, a new class of fluid called "Nanofluid" with enhanced thermo-physical properties are proposed in thermal systems. A nanofluid is a suspension of nanometer sized metal, metal oxide particle or nanotubes in the conventional heat transfer fluids [2].

In the last few decades, large number of investigations were reported which focus on the preparation, characterization and measurement of thermo-physical properties of nanofluids and were summarised in Ghadimi et al. [3]. The measuring of the thermal conductivity and viscosity of nanofluid is considered important as these properties directly influence fundamental heat transfer processes such as natural convection. Literature related to the enhancement in thermal conductivity of various nanofluids was reviewed [4], all of which confirm that the addition of nanoparticles in the fluids enhances the thermal conductivity. The viscosity of nanofluids

was also increased with increasing the nanoparticles which is not desirable for heat transfer applications as it affects the buoyancy movement of fluids. Therefore, literatures related to the measurements of viscosity, model development and numerical analysis of the viscosity of nanofluids are reviewed [5]. It was found that the nanoparticle parameters such as volume fraction, size, shape, and other factors such as temperature and pH were the major factors affecting the viscosity. Apart from the above factors, the presence of a magnetic field also plays a major role in thermo-physical properties especially in thermal conductivity and viscosity [6-8]. Though these effects influence the thermo-physical properties of nanofluids, the influence of such effects on the heat transfer of practical applications, devices that using nanofluids as coolants are not clear. Therefore considering the necessity of such practical applications, natural convection heat transfer studies in a clear cavity and porous cavity filled with various types of nanofluid are investigated.

From the literature [9-13], it was noticed that natural convection heat transfer was enhanced significantly in clear cavities with the use of nanofluids. Initially, Putra et al. [9] conducted an experimental study on natural convection heat transfer process with water based Al_2O_3 and Cu nanofluids in a horizontal cylindrical enclosure. Experiments were conducted with two different volume concentrations of 1% and 4% nanofluids, respectively. In their study, one side of the cylinder is heated and the other side is cooled and the Rayleigh number is varied between $1x10^6$ to $1x10^9$. It was noticed that the particle density, concentration and

aspect ratio had a significant effect on the natural convection heat transfer. However, paradoxical deterioration in the natural convection heat transfer is observed. Nnanna et al. [10] experimentally studied the heat transfer enhancement process with water based Al_2O_3 nanofluids in a rectangular cavity in which vertical walls are heated and horizontal walls are insulated. Heat transfer performance was assessed systematically by varying the volume fraction (from 0 to 8). In their study, Raleigh number is varied between $2x10^6 \leq Ra \leq 3.4x10^6$. It reveals that the concentration between $0.2\% \leq \phi \leq 2\%$ nanoparticle does not impede the natural convection, instead it enhances the heat transfer rate, while the higher concentration (≥2%) decreases the heat transfer due to the increase in viscosity. Moradi et al. [1] studied the influence of the geometry of a cylindrical enclosure on natural convection heat transfer with water based Al_2O_3 and TiO_2 nanofluids. The effect of inclination angle, aspect ratio and heat flux on the natural convection heat transfer was studied. They found that the Al_2O_3 nanofluid enhances the natural convection heat transfer with an optimum concentration of 0.2 Vol% of Al_2O_3. Contrary to this, there was no heat transfer enhancement with the use of TiO_2 nanofluids. Wen and Ding [11] also presented a contradicting result of their study of which decrease in heat transfer coefficient with the increase in TiO_2 nanoparticle concentration. The nanoparticle concentration considered in their study was between $0 \leq \phi \leq 1$, and the Raleigh number was in the range of $1 \times 10^4 \leq Ra \leq 3.5 \times 10^4$ during transient state. In another study, Moradi et al. [12] optimized the natural convection heat transfer by relating the Nusselt

number and Rayleigh number for different concentration of nanofluids subjected to different configurations and orientations of the cylindrical enclosure. The inclination angle, Rayleigh number and volume concentration were varied in the range of $0 \le \theta \le 90$, $1x10^{-8} \le Ra \le 4 \times 10^{-8}$ and $0.1 \le \phi \le 1.5\%$, respectively. It was found that the natural convection heat transfer is enhanced with the use of Al_2O_3 nanofluids and deteriorated while using TiO_2 nanofluids. Very recently, Ghodsinezhad et al. [13] studied the natural heat transfer process in a cavity filled with Al_2O_3/Water nanofluids with the volume concentration varied from $0 \le \phi \le 0.6\%$ and the Raleigh number between $3.49 \times 10^8 \le Ra \le 1.08 \times 10^9$. An optimum of 15% enhancement in heat transfer was found at a volume concentration of 0.1% of Al_2O_3 and further increase in concentration leads to the deterioration of natural convection heat transfer.

Considering the benefits with the possible use of nanofluids in many industrial systems, natural convection heat transfer studies with nanofluid in the porous cavities are initiated and large numbers of numerical studies were performed [14-24]. Buongiorno [14] summarized the slip mechanisms that act on the nanoparticles whilst moving into the base fluids. These are inertia, Brownian diffusion, thermophoresis, diffusiophoresis, Magnus effect, fluid drainage and gravity. Out of this seven slip mechanisms, Brownian diffusion and thermophoresis are concluded to be the two important slip mechanisms and based on this, a two-component four-equation nonhomogeneous equilibrium model for mass, momentum and heat transport was developed for nanofluids. By using above mentioned

mathematical model, Sheremet and Pop [15] numerically analysed the natural convection heat transfer characteristics in a porous cavity filled with nanofluids. In their study, a Darcy–Boussinesq approximation with Buongiorno nanofluids model [14] was used to solve various parameters involved in the study. The parameters considered in the model were Rayleigh number in the range of $100 \leq Ra \leq 500$, Lewis number between of $1 \leq Le \leq 10$, buoyancy ratio parameter between 0.1 to 0.4, thermophororesis parameter between 0.1 to 0.4 and conductivity ratio between 0.1 to 10. The outcome of the study suggests that high thermophoresis parameter, low Brownian motion parameter, low Lewis and Rayleigh numbers and high thermal conductivity ratio return essential non-homogeneous distribution of the nanoparticles inside the porous cavity. Bourantas et al. [16] studied the natural convection heat transfer process in a square porous cavity filled with nanofluids. In their numerical study, the role of thermo-physical properties on the cooling performance of a cavity is studied using a mesh less technique. Grossan et al. [17] numerically analysed the free convection heat transfer characteristics of a porous cavity filled with nanofluid by including the effects of Brownian motion and thermophoresis effect. Also the effect of Rayleigh number, Lewis number and the dimensionless ratio between the thermophoretic and Brownian coefficients on the velocity were studied. Analysis was performed with Rayleigh numbers in the range between $10 \leq Ra \leq 1000$. Their study reveals that the nanofluids in the porous medium reduces the temperature and enhances the heat transfer when the thermal conductivity of the

nanoparticle was much higher than the thermal conductivity of porous material.

Sheremet et al. [18] studied the natural convection heat transfer in a porous cavity filled with nanofluid using the thermal non-equilibrium model along with nanofluids model for thermophyscial properties developed by Tiwari and Das, referred as the Tiwari and Das nanofluids model. In their study, Rayleigh number, porosity, volume fraction and nanofluids/solid matrix interface heat transfer parameters were varied in the range of $10 \leq Ra \leq 100$, $0.1 \leq \varphi \leq 0.9$, $0 \leq \phi \leq 0.05$ and 1 to 1000, respectively. Results showed that the addition of nanoparticles into the base fluid, suppresses the natural convection process. In another study, Sheremet et al. [19] studied the natural convection heat transfer process in a porous cavity filled with nanofluids using Buongiorno's mathematical model, including the two important slip modes Brownian motion and thermophoresis. Results showed that the heat transfer coefficient at the hot side of the cavity is increasing with Brownian motion parameter and decreasing with thermophoresis parameter. Esfandiary et al. [20] numerically investigated the natural convection heat transfer with the use of Al_2O_3 nanofluid in a porous filled cavity including the slip mechanisms such as Brownian motion and thermophorosis using single phase and two phase approach. In their study, inclination angle of cavity was varied from $0 \leq \theta \leq 60^o$, volume fraction was varied between $0 \leq \phi \leq 3\%$ and Rayleigh number was varied between $10^5 \leq Ra \leq 10^7$. Their results showed that by increasing the nanoparticles in the base fluid decreases the Nusselt number at all

concentration of nanofluids. Ghalambaz et al. [21] numerically studied the effects of viscous dissipation and radiation on the natural convection heat transfer in a square cavity filled with porous media and nanofluids. Their results showed that the viscous dissipation affects the Nusselt number in the hot and cold walls of the cavity. Bagheri et al. [22] studied the effect of drag, lift, Brownian and thermophoresis effects on the particle trajectories in the differentially heated cavity. It is noticed that the thermophorosis effects and Rayleigh number has significant effect on the particle deposition and heat transfer.

In order to see the effect of Brownian motion on the effective thermal conductivity and viscosity, Sheikholeslami et al. [23] conducted a three dimensional mesoscopic simulation by including magnetic field effect in natural convection process. They noticed that the application of magnetic field decreases the velocity as the applied magnetic field develops a force that is opposite to fluid flow and creates a drag leading to reduction in convection currents. Ellahi et al. [24] studied the natural convection process including magneto-hydrodynamics effect in nanofluids containing SWCNT and MWCNT suspended in salt water solution. It reveals that the heat transfer is enhanced by increasing the volume fraction of nanotubes, Raleigh number, thermal conductivity of nanolayer and the salt composition in water. Apart from the above cited studies, numbers of works [25-36] were published related to convection process in which flow occurs over different structures with different nanofluids subjected with and without magnetic field.

From the literature review it is evident that the nanofluids and external effect such as magnetic field has a significant effect on the natural convection heat transfer process in cavities. Also, it is noticed that few slip mechanisms such as Brownian motion and thermophoresis effects were added in the numerical studies while other slip mechanisms were ignored. Apart from the slip mechanisms, different analytical models were also used to predict the thermo-physical properties of nanofluids. As a result of the omission of some of the slip mechanisms and the fact that analytical models were used for the prediction of thermo-physical properties, the numerical results of natural convection studies may deviate from the experimental studies. Therefore, experimental studies are needed to predict the natural convection heat transfer and to validate those numerical studies. Grobler et al. [37] studied the natural convection heat transfer in a porous cavity filled with a mixture of 60% Ethylene glycol and 40% Water/Al_2O_3 nanofluids. In their study only one volume concentration of nanofluid (0.2 Vol %) is used and further study is needed to explain the effects of concentration of nanoparticles on the convection heat transfer. Therefore, considering all the factors cited above, natural convection in porous cavity filled with nanofluid is studied with various concentrations of nanoparticles. The main objectives of the present study are to analyse the effect of porosity on the heat transfer ability of cavity, the effect of maintaining the temperature difference (ΔT) of cavity on the heat transfer coefficient of both sides (hot and cold), effect of volume concentration on the Nu, and the effect of Ra on the Nu. The concentration of the nanofluid is varied between $0.05 \leq \phi \leq 0.4\%$.

2. Experimental details

2.1 Preparation of Nanofluids

A stable, concentrated Al_2O_3 (alpha) nanofluid stabilised with polyvinylpyrrolidone (PVP) from US Nanomaterial Research (USA) is procured and diluted with the base fluid. The base fluid consists of 60% ethylene glycol (EG) and 40% deionised water. This combination working fluid is selected because of its anti-freezing capability which is essential in many industrial applications. The average particle size of the nanoparticles is 30 nm. The proportion of EG, water and nanoparticles are determined for different volume concentrations of the nanofluid (0 - 0.4%) and mixed using an ultrasonic processer (Qsonica-Q700) with the processing time of 30 min. To cross check the stability of the nanofluid, UV-visible spectroscopy (Jenway-7315) readings and viscosity at constant temperature are taken. To check the visual stability of the nanofluids, photo graph of both base fluid and nanofluid (at 0.4% volume concentration) is taken immediately after the preparation and after once week of preparation.

2.2 Thermo-physical Properties of nanofluids

A parametric study for thermal conductivity models conducted by Sharifpur et al. [37] and investigation of Aybar et al. [4] suggested that most of the correlations developed for thermal conductivity are suitable for nanofluids with volume concentration less that 1 % vol. Therefore, in this study, thermal conductivity of nanofluid is calculated based on the correlation proposed by Sunder et al. [38], since the base fluid (mixture of 60% ethylene glycol and 40% deionized water), nanoparticles (Al_2O_3), particle size (30 nm) and concentration are same as the present study. The

thermal conductivity of the nanofluids at various volume concentrations is estimated using the equation (1) as

$$\frac{k_{nf}}{k_{bf}} = 1.0618 + 10.448\,\phi, \quad (1)$$

The viscosity of the nanofluid is calculated from the correlation proposed by Sunder et al. [39]

$$\frac{\mu_{nf}}{\mu_{bf}} = 1.1216\,e^{77.56\phi}, \quad (2)$$

In order to validate the viscosity obtained from the equation (2), the viscosity of the nanofluid at 0.05% volume concentration is measured at different temperatures using a Sine-Wave Vibro Viscometer (SV-10) and compared with the results of Sunder et al. [39].

The density of the nanofluid is calculated based on the mixing theory reported by Ho et al. [40] as

$$\rho_{nf} = \phi_{nf}\rho_p + (1 - \phi_{nf})\rho_{bf}, \quad (3)$$

where ρ_p is the density of the nanoparticle (ρ_p= 3950 kg/m^3 which is given by the supplier). The density of the base fluid at different temperature is taken from ASRAE hand book [41]. The specific heat and the thermal expansion coefficient of the nanofluids are estimated from equation (4) and (5), respectively as

$$\rho_{nf}C_{P,nf} = \phi_{nf}\rho_p C_{P,p} + (1 - \phi_{nf})\rho_{bf}C_{P,bf}, \quad (4)$$

$$\rho_{nf}\beta_{nf} = \phi_{nf}\rho_p\beta_p + (1 - \phi_{nf})\rho_{bf}\beta_{bf}, \quad (5)$$

The thermal expansion coefficients of EG and water are 5.4 x 10^{-4} and 2.14 x 10^{-4}, respectively. Therefore the thermal expansion coefficient of base

fluid which contains 60% EG and 40% water is 4.09 x 10^{-4}. The thermal expansion coefficient of Al_2O_3 nanoparticles is found in Ho et al. [28] and is 8.46 x 10^{-6}. The thermal expansion coefficient of glass spheres used as porous media is 0.9 x 10^{-5}.

2.3 Experimental set-up and procedure

The experimental system consists of a cavity, data monitoring and recording unit, thermal baths, pressure and flow measurement devices are shown in the Figure 1. The cavity is made up of two heat exchangers at opposite sides and the other two sides and bottom side as well as a lid constructed from 10 mm thick acrylic material. The width, height and length of the cavity are 120, 96 and 103 mm respectively. Both of the heat exchangers are made up of copper and are kept at a distance of 120 mm and on opposite sides of the cavity. Hot and cold water is supplied to the heat exchangers by two constant water circulation bath (Polyscience). The entire cavity is filled with glass spheres of diameter 16 mm. The specification of glass spears filled in the cavity is given in Table 1. Thermocouples are used to monitor and record the temperature signals of which the detailed positions are shown in Figure 2. In the present study, T-Type (OMEGA) thermocouple wires with the thickness of 0.25 mm and an accuracy of ±0.2 ^{o}C (which includes the uncertainty of data logger) are used. Thermocouples are fixed along the width of the cavity to measure the temperature distribution inside the cavity. Three thermocouples are fixed on both the hot and the cold wall to measure the surface temperature. Two thermocouples are fixed on both the inlet and the outlet of the two heat

exchangers (hot and cold) to monitor the temperature of the water entering and leaving the heat exchangers. To monitor the variation in pressure, a digital pressure gauge (Omega, USA) is mounted on the inlet of both heat exchangers. The flow rate is measured using an ultrasonic flow sensor (Burkert-8081) with a range of 0.06 to 200 l/min, mounted on the inlet of both hot and cold side heat exchangers. The accuracy of the flow measurement is given as ≤ 0.01% of full scale reading and 2% of the measuring value. In order to avoid heat loss from the cavity to the surroundings, the entire cavity is wrapped with an 8 mm thick polyurethane sheet and then kept inside the insulation filled box. Thermocouples were connected to data logger and temperature signals were monitored and recorded by a computer.

The cavity is filled with 500 ml of prepared nanofluid which is sufficient to completely saturate the porous materials. The temperature difference (ΔT) between the hot and cold walls is maintained at 50, 40, 30, and 20 ^{o}C, achieved by adjusting the hot side and cold side temperatures as shown in the Table 2. The temperature variations in the hot and cold walls as well as the working fluid is recorded when the temperature difference is kept constant. The system is assumed to be at steady state when the temperature signals are constant for approximately 40 minutes. After this state, the data is recorded.

2.4 Solution methodology

After the temperature readings at different position of the cavity are recorded, the performance of the cavity is accessed with the estimation of

heat transferred, heat transfer coefficient, Nusselt number and Raleigh number. Heat transferred to the nanofluid from the hot wall or the heat supplied at the hot side heat exchanger is calculated using Newton's law of cooling as shown in equation (6)

$$\dot{q_h} = \dot{m}_h \, C_p \, (T_{h,i} - T_{c,o}), \tag{6}$$

Similarly, heat absorbed by the cold side heat exchanger is calculated by the equation (7)

$$\dot{q_c} = \dot{m}_c \, C_p \, (T_{h,o} - T_{c,i}), \tag{7}$$

The heat transfer coefficient at the hot and cold wall is calculated using equation (8) and (9) respectively.

$$h_h = \frac{\dot{q_h}}{(T_h - T_f)}, \tag{8}$$

$$h_c = \frac{\dot{q_c}}{(T_f - T_c)}, \tag{9}$$

The Nusselt number is calculated as,

$$Nu = \frac{h\,l}{k}, \tag{10}$$

The heat transfer coefficient of the cavity is the average heat transfer coefficients of the hot and cold wall (ie $h = (h_h + h_c)/2$). Generally, the Rayleigh number is useful to identify the heat transfer mechanism in the cavity. For a clear cavity the Rayleigh number is given as,

$$Ra_L = \frac{g\,\beta_{bf}\,\rho_{bf}^2\,C_{p,bf}(T_h - T_c)\,L^3}{k_{bf}\,\mu_{bf}}, \tag{11}$$

and the Rayleigh number for a porous cavity filled with a nanofluid is calculated using the temperature difference between the hot and cold side, permeability and cavity dimensions as

$$Ra_L^* = \frac{g\beta_{nf}\,\rho_{nf}^2 C_{p.nf}(T_h - T_c)\,KL_c}{k_{nf}\,\mu_{nf}}, \quad (12)$$

where g is the gravity constant, β is the volumetric expansion coefficient of the fluid, T_h and T_c are the isothermal wall temperatures of the hot and cold sides, respectively. The permeability (K) of the cavity is estimated using the Carman-Kozeny relationship given as,

$$K = \frac{D^2\varphi^3}{180(1-\varphi)^2}, \quad (13)$$

where φ is the porosity of cavity. The porosity and permeability of the porous medium is found to be 0.249 and 3.43×10^{-7} m^2, respectively. Finally, the uncertainty present in the heat transfer rate, heat flux, heat transfer coefficient and Nu are estimated. The uncertainty present in the estimation of heat transfer coefficient and Nu is found to be between 2 to 5 %.

3. Results and Discussion

Figure 3 shows the stability of the nanofluids in terms of the UV-visible absorbance and viscosity of the fluids. The viscosity of 0.4% volume concentration of nanofluid is monitored at a constant temperature of 20 ^oC for 48 hours. It is found that the UV-visible absorbance and the viscosity are unchanged over 48 hours, suggesting that the prepared nanofluid is stable. The visual stability of the nanofluids is also presented in Figure 4

and showed no evidence of sedimentation even after a week. Though the nanofluid is stable for more than a week, the heat transfer experiments are completed within 7 hours from the time of preparation.

The thermal conductivity at different concentration of nanofluid is estimated using equation (1). Similarly, the viscosity of the nanofluid is estimated using equation (2) and to validate this result; the viscosity of the nanofluid is measured. It is found that the measured and estimated viscosities are comparable as shown in Figure 5. Therefore, the same Equation (2) is used to estimate the viscosities of other concentrations of nanofluids. The estimated thermal conductivities and viscosities are used to calculate the Nusselt number.

In order to validate the experimental results obtained, a comparison is made between the average experimental Nu with average analytical Nu. The analytical model proposed by Berkovsky and Polevikov [42] presented in equation 14 is used to predict the Nu.

$$\overline{Nu} = 0.18\left(\frac{Pr}{0.2+Pr}Ra\right)^{0.29}, \qquad (14)$$

Figure 6 shows the comparison between the average experimental Nu with average analytical Nu calculated using equation 14 and it is comparable. Also the experimental measurements are following the same trend of analytical model that confirms the validity of experimental measurements.

Moreover, the Nu variations with ΔT of the clear cavity and porous cavity are calculated using Equation (10) and presented in Figure 7. It is seen that the Nu increases as the ΔT increases for both clear cavity and

porous cavity. As the ΔT increases, the hot wall temperature increases leading to a reduction in the density of the fluid and a subsequent improvement in the buoyancy resulting in a faster upward movement and thus a faster circulation of the fluid. Therefore, the Nu increases with the ΔT increase. It is also seen that the Nu of porous cavity is lower than that of the clear cavity. This is mainly due to the resistance offered by the porous media in the cavity. The porous structure reduces the buoyancy and limits the fluid circulation, which leads to the reduction in Nu number in the porous cavity. Further, the Nu of the clear cavity is in the range of 45 to 59 while the Nu of the porous cavity is in the range of 34 to 45, which is 24% less than that of the clear cavity. Though the porous cavity underperformed compared to the clear cavity, it is necessary to study this type of heat transfer performance due to the large number of industrial applications.

Figure 8 shows the heat transfer capability of nanofluids at different concentrations of nanoparticles in the base fluid for various ΔT. It can be observe that the heat transfer is increased for all volume fractions when the temperature difference increases. It is also shown that the heat transfer capabilities are enhanced through the addition of nanoparticles to the base fluid. At a volume fraction of 0.05%, the heat transfer capability is enhanced by a maximum of 10% compared to the base fluids. This enhancement is mainly due to the enhancement in the thermo-physical properties of the nanofluids. The addition of nanoparticles to the base fluid enhances the thermal conductivity of the working fluid and leads to more heat conduction and quicker heat transfer. This higher heat transfer causes density

variations, leading to higher buoyancy forces which promotes higher circulation of the fluids and enhances the heat transfer ability. Apart from the thermo-physical properties of nanofluids, the transport mechanisms involved between the liquid-solid interface such as Brownian motion and thermophoresis of nanoparticles also influence the heat transfer, especially when the temperature gradient is higher [37]. Moreover, at $\Delta T = 50\ ^{o}C$, the heat transferred by the nanofluid is increased as the concentration increases up to 0.05%, afterwards it is slightly decreased up to 0.3% then it drops further at 0.4%. This trend indicates that an optimum concentration exists for the maximum heat transfer. The maximum heat transferred by nanofluid happened at $\Delta T = 50^{o}C$ which was 54 W at the nanoparticle concentration of 0.05%. Moreover, the heat transfer is decreased as the ΔT decreased while almost uniform heat transfer is found in the concentration range of 0.05 to 0.3% and a further increase in the nanoparticle quantity leads to the decrease in heat transfer.

In order to check the heat transfer efficiency of nanofluids, heat supplied to the hot side heat exchanger and heat transferred by the cold side heat exchanger is compared and presented in Figure 9. It shows that there is a linear increase in heat transfer with the heat supplied. Also, it is noticed that heat transfer capacity is more at higher heat inputs and is less at lower heat inputs. It reveals that the efficiency of the nanofluid is increased at higher heat inputs. This enhancement is due to the enhancement in the thermo-physical properties leading to better fluid circulation due to buoyancy in the cavity.

To analyse whether the heat transfer performance of the cavity is influenced more by the hot wall or the cold wall, the heat transfer coefficients at both walls are calculated at different ΔT and presented in Figure 10. It is seen that the heat transfer coefficient increase linearly with an increase in the ΔT. It is also noticed that the heat transfer coefficient of 0.05 vol% Al_2O_3 nanofluid is higher than that of all the other concentrations, including the base fluid. Further 0.05%, it is observed that the heat transfer coefficient decreases as the concentration increases from. Eventhough the heat transfer coefficients of the nanofluids with volume fractions of 0.1 to 0.3% decrease as the concentration increases, these heat transfer coefficients are still higher than the heat transfer coefficient of the basefluid. This enhancement may be due to the increase in Brownian motion in the fluid as the ΔT increases, as reported by Sheremet et al [19]. However, the heat transfer coefficient of the 0.4% volume concentration nanofluid is lower than the heat transfer coefficient of basefluid.

The heat transfer coefficient at the cold wall is presented in Figure 11 and it increases with ΔT similar to the heat transfer coefficient in the hot wall. Contrary to the heat transfer coefficient at the hot wall, however, the heat transfer coefficient in the cold wall behaves differently. At the nanoparticle volume concentration of 0.05%, the heat transfer coefficient is higher than that of the base fluid and it is deteriorated at higher concentration of nanofluids. Moreover, the effect of the temperature difference on the heat transfer coefficient at the cold wall is significant at lower ΔTs and less significant at higher ΔT values. This variation is mainly

because of the variation in temperature of the cold wall and the hot wall. At higher ΔT of 50 ^{o}C, the cold wall temperature is 5 ^{o}C and the hot wall temperature is 55 ^{o}C, resulting in a higher heat transfer coefficient in the hot wall and a lower heat transfer coefficient in the cold wall. On the other hand, when the ΔT is 20 ^{o}C, the hot wall temperature is 40 ^{o}C and the cold wall temperature is 20 ^{o}C leading to a significant variation in the heat transfer coefficient at lower ΔT values. Therefore, the temperature has a significant effect on the heat transfer coefficient at the cold wall. It is known that the thermal conductivity of a nanofluid increases with temperature. Therefore, the heat transfer coefficient at the hot wall is always higher while the same at the cold wall is lower due to the low thermal conductivity resulting from the low temperature.

The average Nu of the cavity at different nanofluid volume concentration is presented in Figure 12. It shows that the average Nusselt number increases with an increase in ΔT for all concentrations as well as the base fluid. However, as the volume concentration increases, the average Nu is increased at 0.05 vol% then it decreased gradually as the volume fraction increases. It is also noticed that the Nu of the 0.1 to 0.4% volume concentration of nanofluids, is lower than that of the Nu of the base fluids. As the volume concentration increases, the density and the viscosity of the nanofluid increase, leading to a decrease in the buoyancy forces resulting in less vertical movement of the fluid which affects fluid circulation and reduces the heat transfer. A similar observation is found in the literature [40]. Apart from the previously mentioned reason, as can be seen in Figure

(9) and (10), the performance reduction is due to the negative effect in the heat transfer coefficient and the temperature in the cold wall. This may be due to the thermophoresis effect. As the ΔT increases, due to the movement of the nanoparticles from the hot side to the cold side, there is a thin layer of low concentration nanofluid near the hot wall and a thin layer of high concentration nanofluid near the cold wall is created. Therefore, due to the buoyancy the low concentration fluid fills the top portion of the cavity and high concentration fluid fills the bottom portion of the cavity. As a result of this formation, this fluid in the top and bottom region of cavity escapes from the bulk fluid movement and creates less effective space leading to low heat transfer [41]. This negative effect in the cold wall is higher than the positive effect in the hot wall leading to the lower Nu.

The Rayleigh number (Ra) is useful to study the effect of buoyancy on the heat transfer performance of the cavity. Figure 13 shows the relation between Nu and Ra for the clear cavity filled with the base fluid, porous cavity with base fluid and the porous cavity with various concentrations of nanofluids. In all cases, it is seen that the Nu increases as the Ra increases. It suggests that the buoyancy force increases with the ΔT increase, resulting in an increase in the fluid circulation in the cavity leading to an enhancement in Nu. The clear cavity filled with base fluid showed a higher Nu number compared to porous cavity filled with base fluid as well as nanofluid. It is noted that the Ra of clear cavity is in the range of $1.4 \times 10^8 \leq Ra \leq 3.5 \times 10^8$ while the Ra of porous cavity is in the range of $3 \times 10^3 \leq Ra \leq 1.2 \times 10^4$. The main reason for this variation is the permeability change as a

result of filling the cavity with porous material. The presence of porous materials restrains the buoyancy and leads to low fluid circulation resulting in a low Nu number. It is also noticed that the Rayleigh numbers of the nanofluids are lower than the Rayleigh number of the base fluids except for the nanofluid with 0.05 volume concentration. These negative effects are caused by the effects of low temperature at the cold wall as discussed earlier.

Conclusion

Experiments were performed to investigate the effect of porous medium and nanofluid on the heat transfer capabilities of buoyancy driven flow in a differentially heated square cavity. The results showed that heat transfer is affected by both the porous medium and the nanofluids and their volume fraction. The clear cavity (just base fluid without porous media) transferred the highest amount of heat whilst the least amount of heat was transferred by the porous medium saturated with base fluid or with 0.4 Vol% nanofluid. The nanoparticle volume concentration of 0.05% is found to be the optimum for maximum heat transfer as that nanofluid transfers 10% more heat compared to the base fluid in the porous cavity. It was found that the temperature at the cold side of the cavity has a significant effect on the Nu and heat transfer ability of cavity.

References

[1]. H. Moradi, B. Bazooyar, S.G. Etemad, A. Moheb, Influence of the geometry of cylindrical enclosure on natural convection heat transfer of Newtonian nanofluids, Chemical Engineering Research and Design 94 (2015) 673-680.

[2]. S.U.S. Choi and J.A. Eastman, Enhancing thermal conductivity of fluids with nanoparticles, ASME Mechanical Engineering Congress & Exposition, Nov 12-17, 1995, Sanfrancisco.

[3]. A. Ghadimi, R. Saidur and H.S.C. Metselaar, A review of nanofluid properties and characterization in stationary conditions, International Journal of Heat and Mass Transfer 54 (2011) 4051-4068.

[4]. H.Ş. Aybar, M. Sharifpur, M.R. Azizian, M. Mehrabi, and J.P. Meyer, A Review of Thermal Conductivity Models of Nanofluids, Heat Transfer Engineering 36 (13) (2015) 1085-1110.

[5]. J.P. Meyer, S.A. Adio, M. Sharifpur and P.N. Nwosu, The viscosity of nanofluids: a review of the theoretical, empirical, and numerical models, Heat Transfer Engineering (2015).

[6]. A. Shahsavar, M.R. Salimpour, M. Saghafian and M.B. Shafii, Effect of magnetic field on thermal conductivity and viscosity of a magnetic nanofluid loaded with carbon nanotubes, Journal of Mechanical Science and Technology 30 (2) (2016) 809-815.

[7]. D. Song, D. Jing, J. Geng, Y. Ren, A modified aggregation based model for the accurate prediction of particle distribution and viscosity in magnetic nanofluids, Powder Technology 283 (2015) 561–569.

[8]. D. Song, D. Jing, B. Luo, J. Geng, and Y. Ren, Modeling of anisotropic flow and thermodynamic properties of magnetic nanofluids induced by external magnetic field with varied imposing directions, Journal of Applied Physics 118 (2015) 045101.

[9]. N. Putra, W. Roetzel, S. Das, Natural convection of nano-fluids, Heat and Mass Transfer 39 (2003) 775-784.

[10]. A.G. Nnanna, Experimental model of temperature-driven nanofluid, Journal of Heat Transfer 129 (2006) 697-704.

[11]. D. Wen, Y. Ding, Formulation of nanofluids for natural convective heat transfer applications, International Journal of Heat and Fluid Flow 26 (2005) 855 – 864.

[12]. H. Moradi, B. Bazooyar, A. Moheb, S.G. Etemad, Optimization of natural convection heat transfer of Newtonian nanofluids in a cylindrical enclosure, Chinese Journal of Chemical Engineering 23 (2015) 1266-1274.

[13]. H. Ghodsinezhad, M. Sharifpur, J.P. Meyer, Experimental investigation on cavity flow natural convection of Al_2O_3–water nanofluids, International Communications in Heat and Mass Transfer 76 (2016) 316 - 324.

[14]. J. Buongiorno, Convective Transport in Nanofluids, ASME Journal of Heat Transfer 128 (2006) 240-250.

[15]. M.A. Sheremet, I. Pop, Conjugate natural convection in a square porous cavity filled by a nanofluid using Buongiorno's mathematical model, International Journal of Heat and Mass Transfer 79 (2014) 137–145.

[16]. G.C. Bourantas, E.D. Skouras, V.C. Loukopoulos, V.N. Burganos, Heat transfer and natural convection of nanofluids in porous media, European Journal of Mechanics B/Fluids 43 (2014) 45–56.

[17]. T. Grossan , C. Revnic , I. Pop , D.B. Ingham, Free convection heat transfer in a square cavity filled with a porous medium saturated by a nanofluid, International Journal of Heat and Mass Transfer 87 (2015) 36 – 41.

[18]. M.A. Sheremet, I. Pop, R. Nazar, Natural convection in a square cavity filled with a porous medium saturated with a nanofluid using the thermal non equilibrium model with Tiwari and Das nanofluid model, International Journal of Mechanical Sciences 100 (2015) 312 – 321.

[19]. M.A. Sheremet, I. Pop, M.M. Rahman, Three-dimensional natural convection in a porous enclosure filled with a nanofluid using Buongiorno's mathematical model, International Journal of Heat and Mass Transfer 82 (2015) 396 – 405.

[20]. M. Esfandiary, B. Mehmandoust, A. Karimipour, H.A. Pakravan, Natural convection of Al_2O_3 water nanofluid in an inclined enclosure with the effects of slip velocity mechanisms: Brownian motion and thermophoresis phenomenon, International Journal of Thermal Sciences 105 (2016) 137-158.

[21]. M. Ghalambaz , M. Sabour, I. Pop, Free convection in a square cavity filled by a porous medium saturated by a nanofluid: Viscous dissipation and radiation effects, Engineering Science and Technology, an International Journal 19 (2016) 1244 - 1253.

[22]. G.H. Bagheri, M. Salmanzadeh, V. Golkarfard, and G. Ahmadi, Simulation of solid particles behaviour in a heated cavity at high Rayleigh numbers, Aerosol Science and Technology 46 (2012) 1382 - 139.

[23]. M. Sheikholeslami, R. Ellahi, Three dimensional mesoscopic simulation of magnetic field effect on natural convection of nanofluids, International Journal of Heat and Mass Transfer 89 (2015) 799 - 808.

[24]. R. Ellahi, M. Hassan, and A. Zeeshan, Study of natural convection MHD nanofluid by means of single and multi-walled carbon

nanotubes suspended in a salt-water solution, IEEE Transactions on Nanotechnology 14 (4) (2015) 726 - 734.

[25]. N. S. Akbar, M. Raza, R. Ellahi, Copper oxide nanoparticles analysis with water as base fluid for peristaltic flow in permeable tube with heat transfer, computer methods and programs in biomedicine 130 (2016) 22 - 30.

[26]. N. S. Akbar, M. Raza, R. Ellahi, Influence of induced magnetic field and heat flux with the suspension of carbon nanotubes for the peristaltic flow in a permeable channel, Journal of Magnetism and Magnetic Materials 381 (2015) 405 - 415.

[27]. M. Khazayinejad, M. Hatami, D. Jing, M. Khaki, G. Domairry, Boundary layer flow analysis of a nanofluid past a porous moving semi-infinite flat plate by optimal collocation method, Powder Technology 301 (2016) 34 - 43.

[28]. A. Zeeshan, A. Majeed, R. Ellahi, Effect of magnetic dipole on viscous ferro-fluid past a stretching surface with thermal radiation, Journal of Molecular Liquids 215 (2016) 549 - 554.

[29]. M. Hatami, M. Khazayinejad, D. Jing, Forced convection of Al_2O_3–water nanofluid flow over a porous plate under the variable magnetic field effect, International Journal of Heat and Mass Transfer 102 (2016) 622 - 630.

[30]. R. Ellahi, M. Hassan and A. Zeeshan, Aggregation effects on water base Al_2O_3-nanofluid over permeable wedge in mixed convection, Asia-Pacific Journal of Chemical Engineering 11 (2016) 179 -186.

[31]. N. S. Akbar, M. Raza, R. Ellahi, Impulsion of induced magnetic field for Brownian motion of nanoparticles in peristalsis, Applied Nano science 6 (2016) 359 - 370.

[32]. R. Ellahi, M. Hassan, A. Zeeshan, Shape effects of nanosize particles in Cu—H_2O nanofluid on entropy Generation, International Journal of Heat and Mass Transfer 81 (2015) 449 - 456.

[33]. S.U. Rahman, R. Ellahi, S. Nadeem, Q.M. Zaigham Zia, Simultaneous effects of nanoparticles and slip on Jeffrey fluid through tapered artery with mild stenosis, Journal of Molecular Liquids 218 (2016) 484 - 493.

[34]. S. Rashidi, M. Dehghan, R. Ellahi, M. Riaz, M.T. Jamal-Abad, Study of stream wise transverse magnetic fluid flow with heat transfer around an obstacle embedded in a porous medium, Journal of Magnetism and Magnetic Materials 378(2015)128 - 137.

[35]. R. Ellahi, M. Hassan, A. Zeeshan, A. A. Khan, The shape effects of nanoparticles suspended in HFE-7100 over wedge with entropy generation and mixed convection, Applied Nano science 6 (2016) 641 - 651.

[36]. C. Grobler, M. Sharifpur, H. Ghodsinezhad, R. Capitani and J.P. Meyer, Experimental study on cavity flow natural convection in a porous medium, saturated with an Al_2O_3 60%EG-40% Water nanofluid, 11th International Conference on Heat Transfer, Fluid Mechanics and Thermodynamics.

[37]. M. Sharifpur, T. Ntumba, J.P. Meyer, Parametric analysis of effective thermal conductivity models for nanofluids, ASME 2012 International Mechanical Engineering Congress and Exposition 9 (2012) , Paper No. IMECE2012 - 85093.

[38]. L.S. Sundar, E.V. Ramana, M.K. Singh, A.C.M. Sousa, Thermal conductivity and viscosity of stabilized ethylene glycol and water mixture Al_2O_3 nanofluids for heat transfer applications: An experimental study, International Communications in Heat and Mass Transfer 56 (2014) 86 - 95.

[39]. C.J. Ho, W.K. Liu, Y.S. Chang, and C.C Lin, Natural convection heat transfer alumina – water nanofluid in vertical square enclosures: An experimental study, International Journal of Thermal Sciences 49 (2010) 1345 - 1353.

[40]. Ashrae, *Ashrae Handbook Fundamentals*, American Society of heating, Refrigerating and air conditioning Engineers, 2009.

[41]. H. Aminfar and M.R. Haghgoo, Brownian motion and thermophoresis effects on natural convection of alumina-water nanofluid, Journal of Mechanical Engineering Science 227 (2012) 100 -110.

[42]. B. Berkovsky, V. Polevikov, Numerical Study of Problems on High-intensive Free Convection, Proceedings of International Turbulent Buoyant Convection Seminar, 1977. (http://www.elib.bsu.by/handle/123456789/10278).

Nomenclature

C_p specific heat,

D diameter,

g acceleration due to gravity,

h heat transfer coefficient,

k thermal conductivity,

K permeability,

l characteristic length,

$\dot{m}$ mass flow rate,

Nu Nusselt number

$\dot{q}$ heat flux,

Ra Raleigh number

T temperature,

Greek symbols

φ porosity

μ viscosity,

β thermal expansion coefficient

ρ density,

Subscripts

bf base fluid

c cold

f fluid

h hot

i inlet

nf nanofluid

o outlet

Figure captions

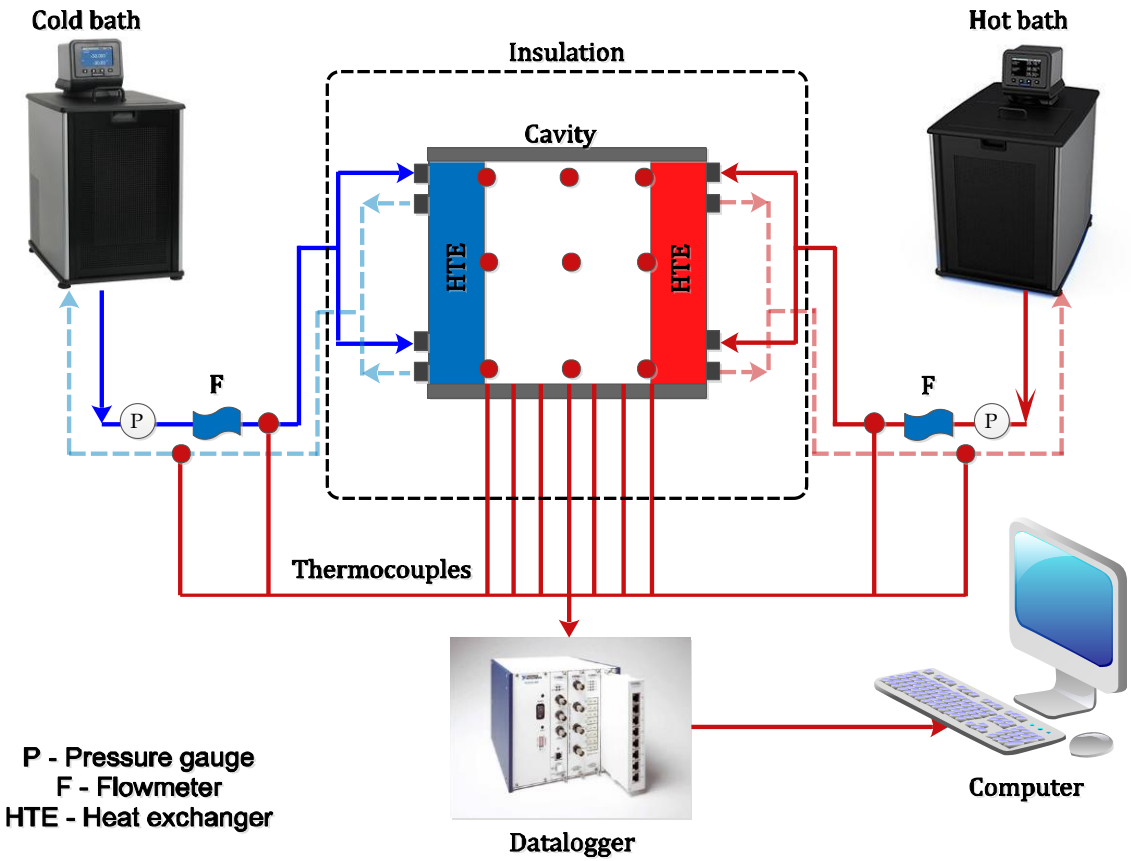

Figure 1 Schematic view of Experimental set-up

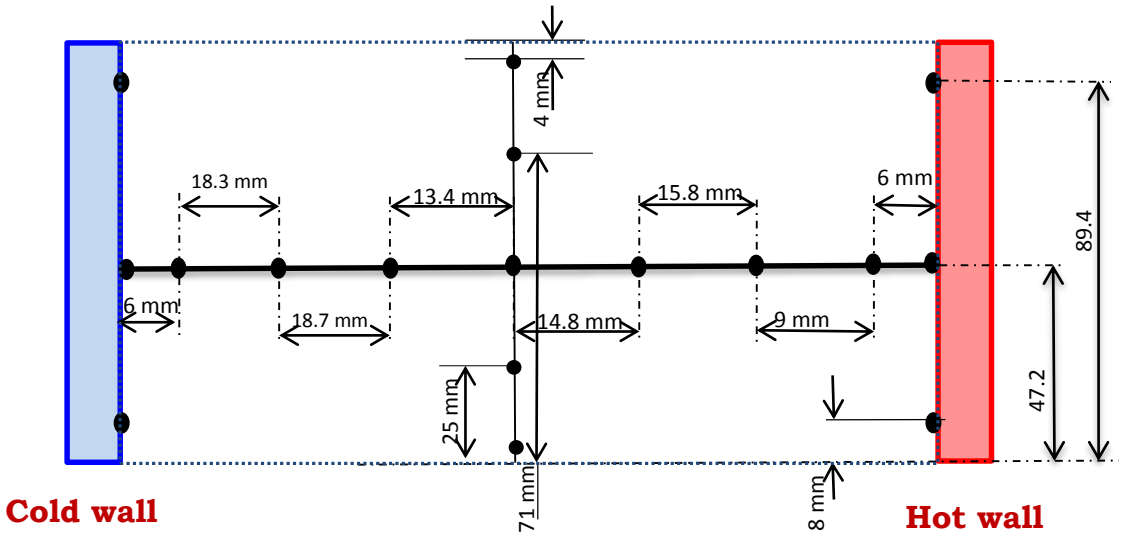

Figure 2. Positions of Thermocouples

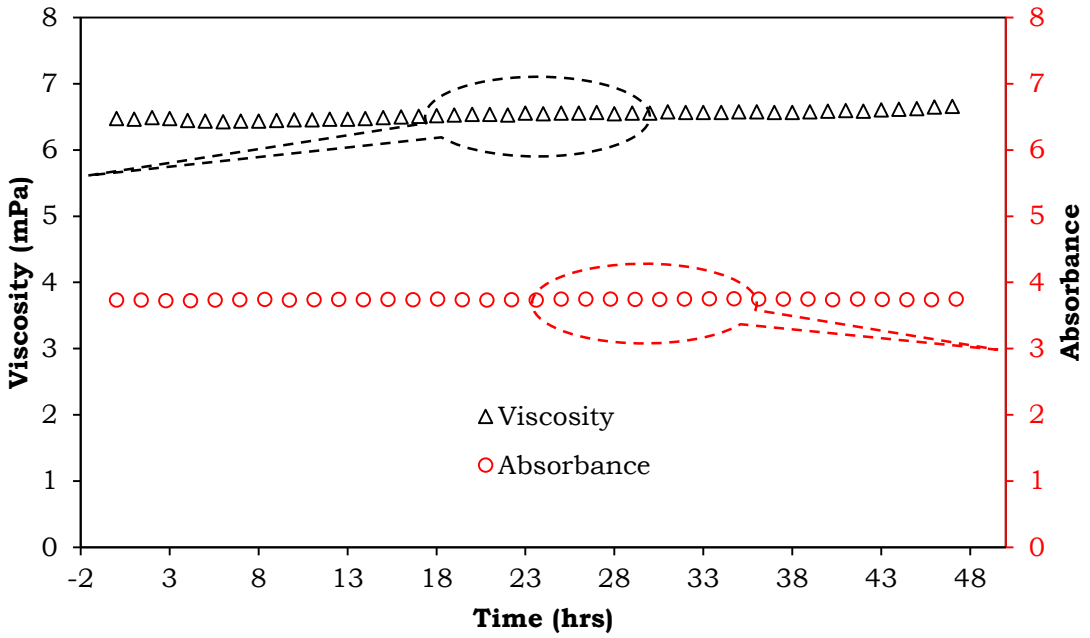

Figure 3 Viscosity and Absorbance of 0.4 vol% nanofluid at 20 °C

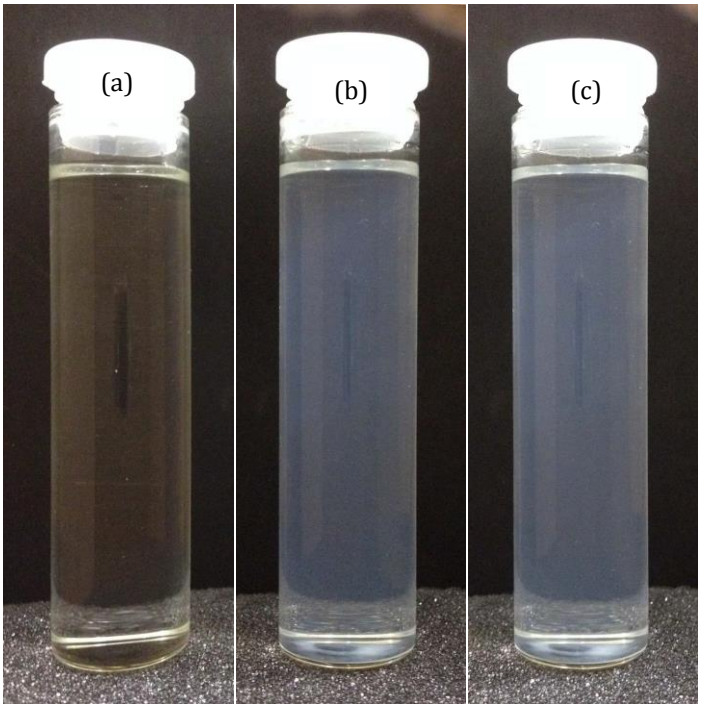

Figure 4 Stability of (a) Base fluid and (b) 0.4 vol% Al_2O_3 nanofluid immediately after preparation (c) after a week

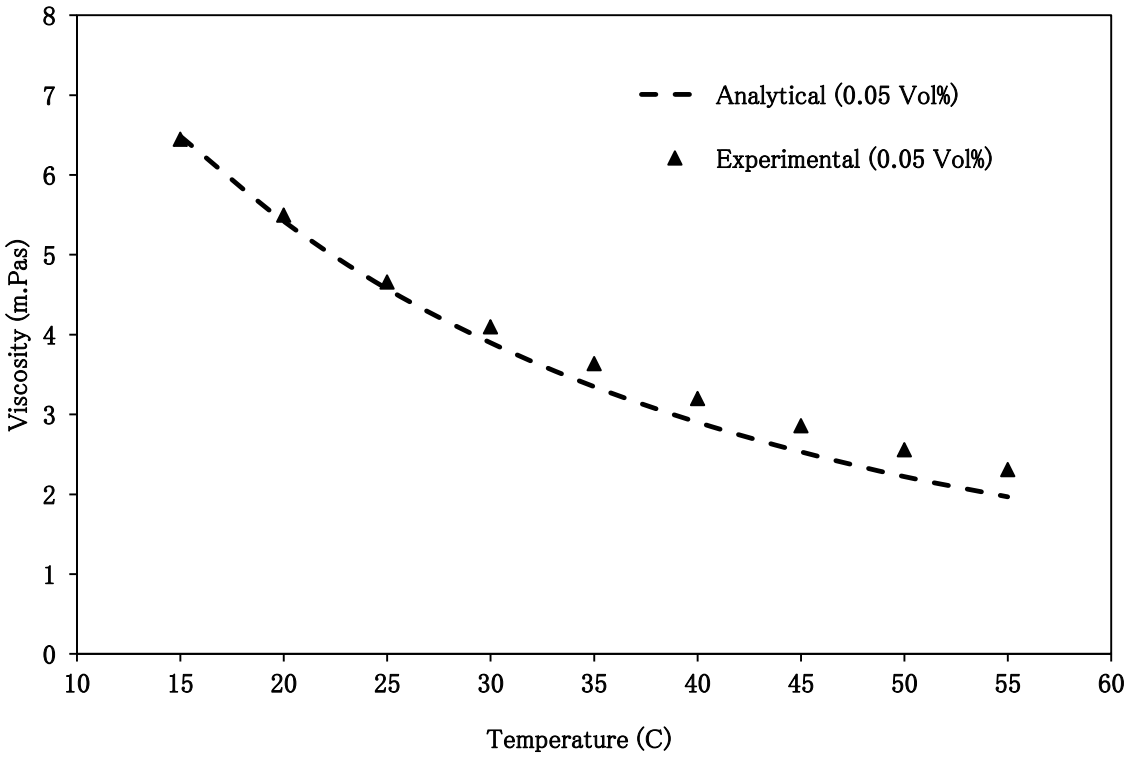

Figure 5. Comparison of measured and predicted [22] viscosity at 0.05 volume concentration

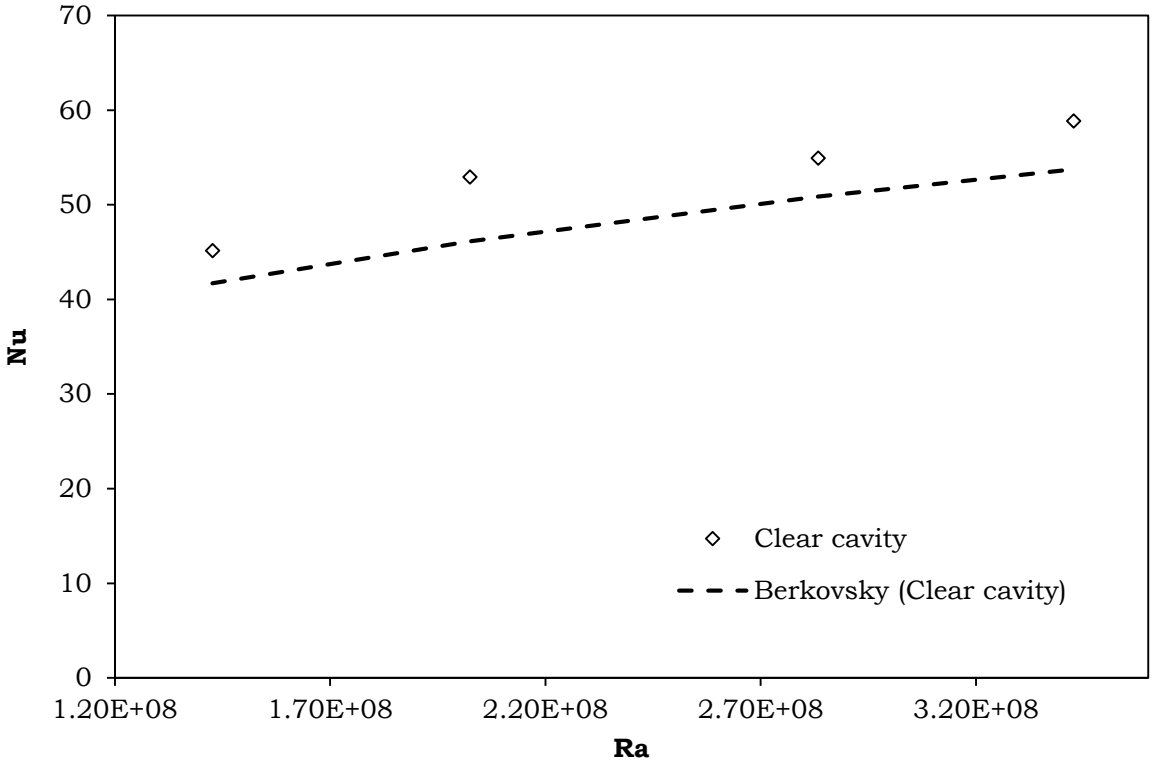

Figure 6. Validation of experimental Nu with analytical Nu for clear cavity with base fluid

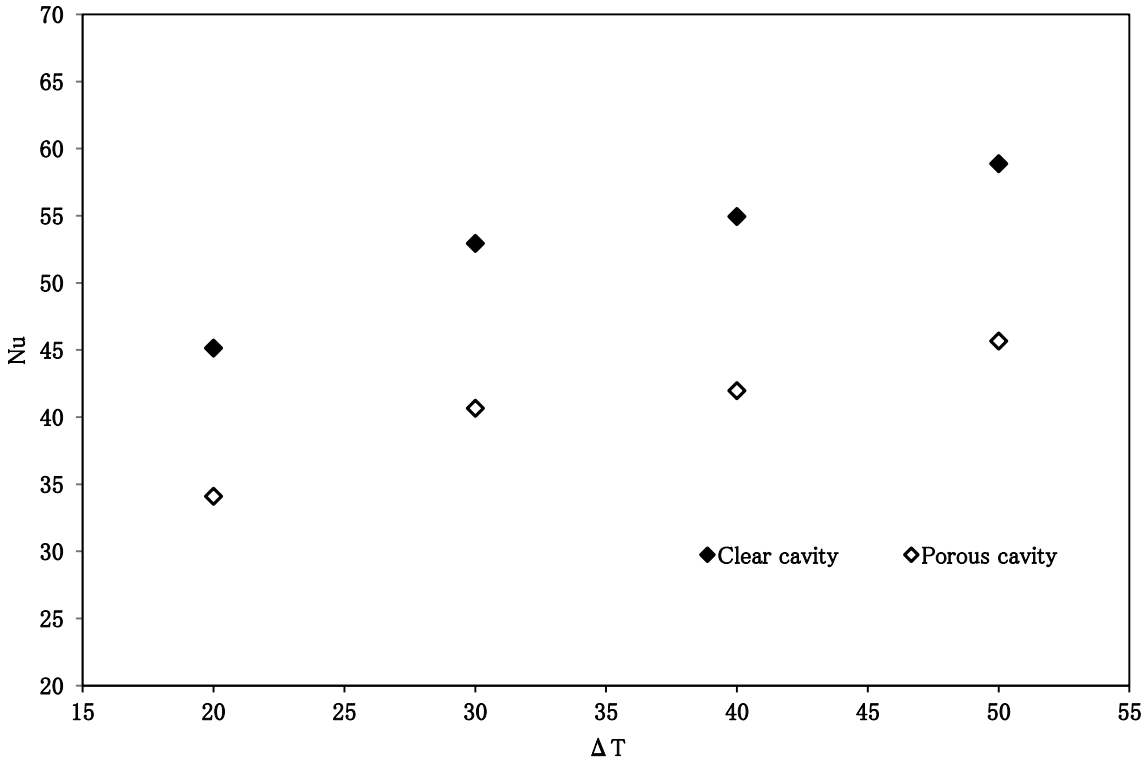

Figure 7. Nu number variations in Clear cavity and porous cavity

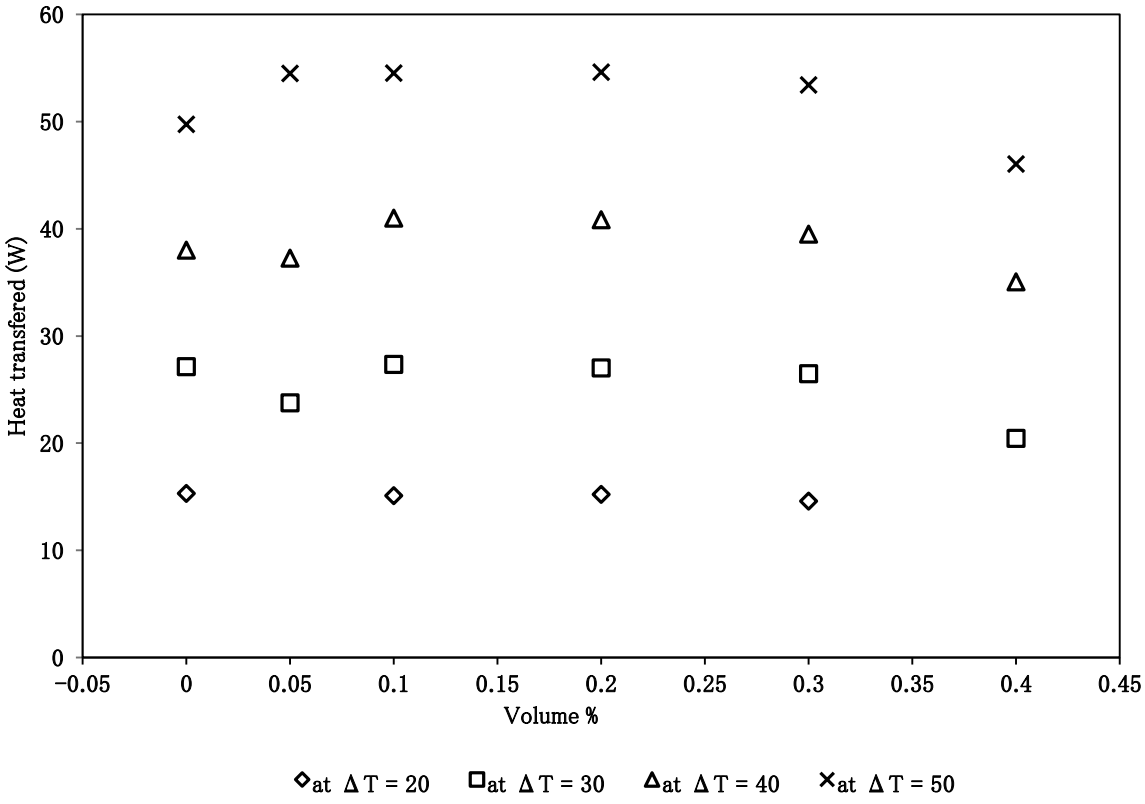

Figure 8. Heat transferred by nanofluids with porous cavity at different temperature differences for various concentrations of nanofluids

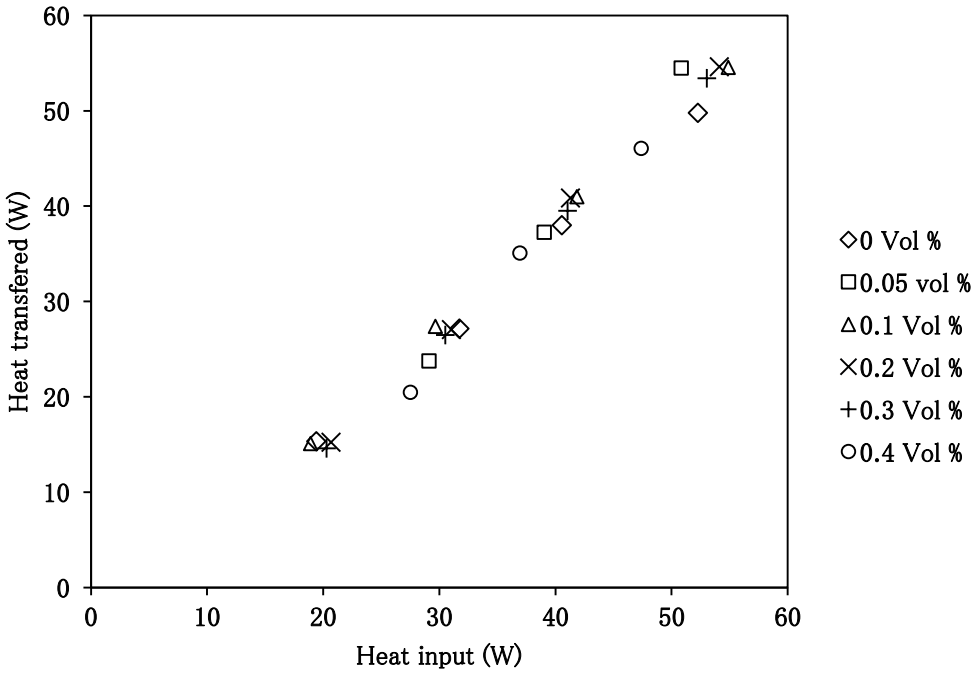

Figure 9. Heat Transfer performance of porous cavity filled with nanofluids

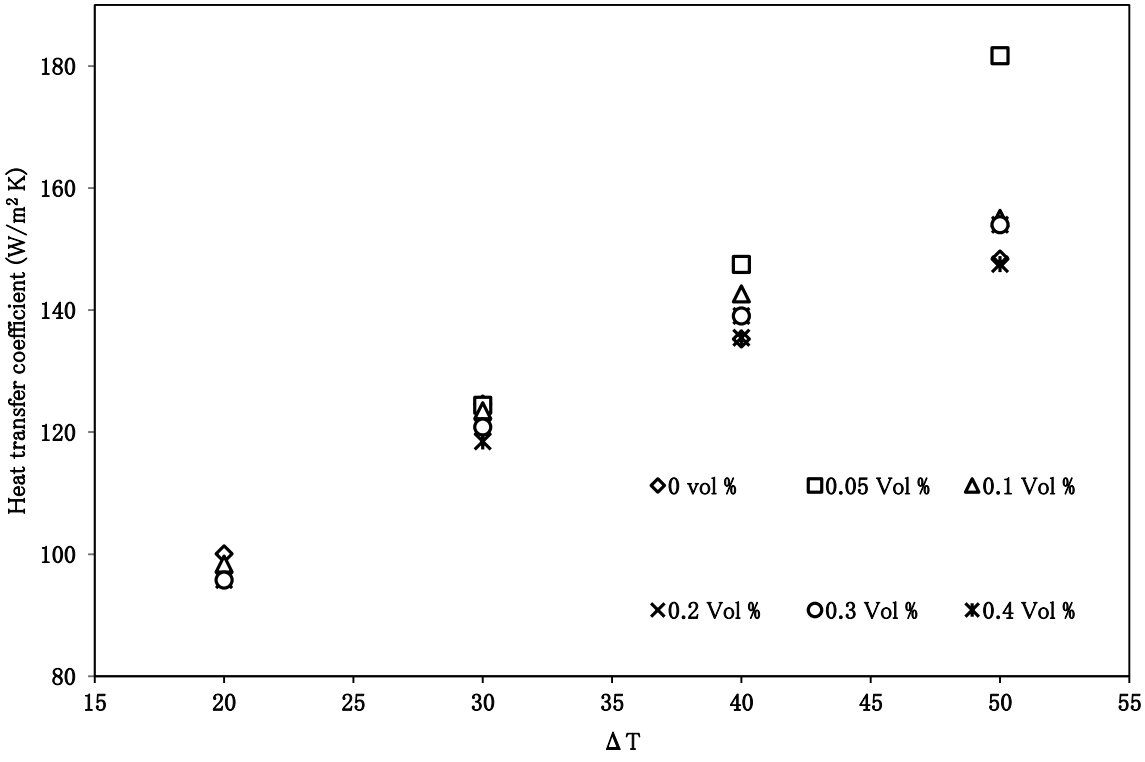

Figure 10. Heat transfer coefficient at the hot side of the porous cavity

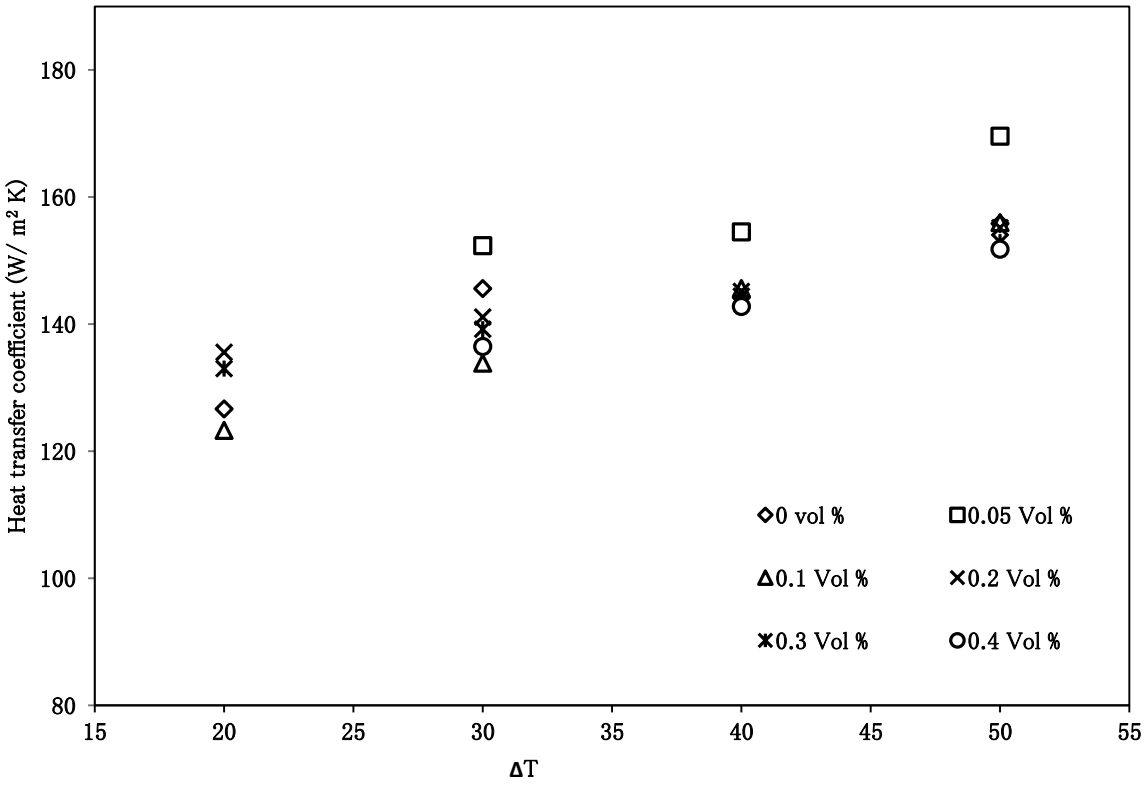

Figure 11. Heat transfer coefficient at the cold side of the porous cavity

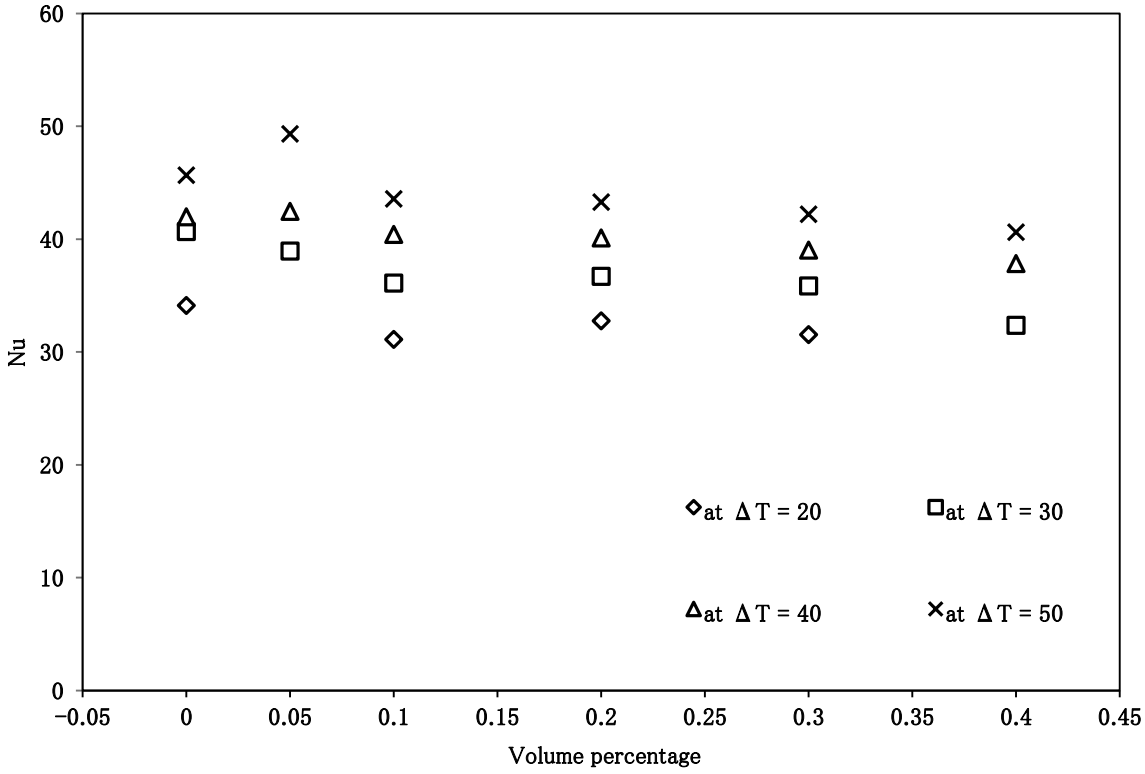

Figure. 12 Average Nu number variations at different concentrations of nanofluids in the porous cavity

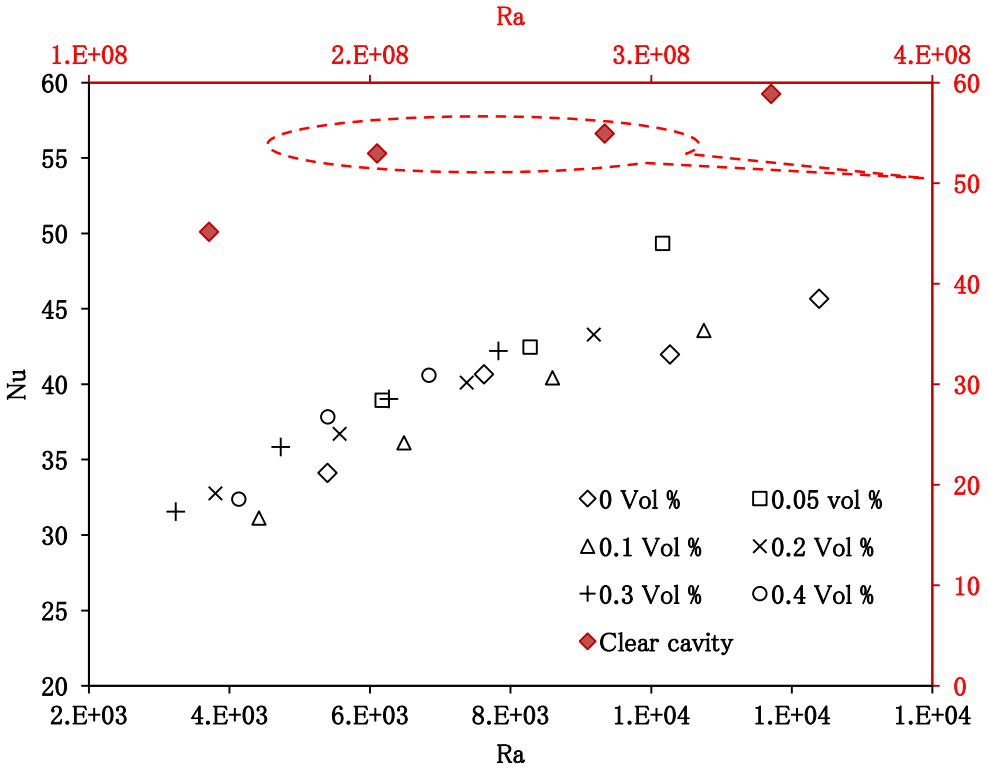

Figure 13. Average Nu number variations at different Ra number of both clear cavity and porous cavity

Table 1: Material Properties of the Porous Media

Property	Value
Sphere diameter	16 mm
Thermal Conductivity	0.7 W/m-K
Density	2800 kg/m^3
Specific Heat	13.96 J/kg-K

Table 2: Testing conditions

Hot side temperature	Cold side temperature	Temperature difference
55	5	50
50	10	40
45	15	30
40	20	20